Hindawi Publishing Corporation
Journal of Nanomaterials
Volume 2016, Article ID 8970213, 12 pages
http://dx.doi.org/10.1155/2016/8970213

Research Article

Medicated Nanofibers Fabricated Using NaCl Solutions as Shell Fluids in Modified Coaxial Electrospinning

Yong-Hui Wu,[1] Chen Yang,[2] Xiao-Yan Li,[2] Jia-Ying Zhu,[2] and Deng-Guang Yu[2]

[1]*Department of Mechanical Engineering, Guangxi Technological College of Machinery and Electricity, Nanning 530007, China*
[2]*School of Material Science and Engineering, University of Shanghai for Science and Technology, Shanghai 200093, China*

Correspondence should be addressed to Deng-Guang Yu; ydg017@usst.edu.cn

Received 4 December 2015; Accepted 22 March 2016

Academic Editor: Marco Salerno

The present study reports the fabrication of medicated nanofibers for potential colon-targeted drug delivery using modified coaxial electrospinning, in which salt (NaCl) solutions were exploited as shell fluids to facilitate the preparation processes. A homemade concentric spinneret with an indented core capillary was developed to conduct the coaxial processes. Optical observations and scanning electron microscopic results demonstrated that the shell-to-core fluid flow rate ratio was a key parameter, which exerted a significant influence on the electrospinning processes and could be exploited to control the fibers' morphology and diameters. A scaling law of $D = 0.173F^{-0.531}$ ($R^2 = 0.9976$) was built, by which the nanofibers' sizes can be predicted and manipulated easily. X-ray diffraction and attenuated total reflected FTIR tests verified that the medicated nanofibers were essentially a polymeric nanocomposite and the guest drug diclofenac sodium (DS) had fine compatibility with the host polymer. All the drug was encapsulated in the filament-forming carrier. *In vitro* dissolution experiments demonstrated that the medicated nanofibers could free the drug in a neutral condition, suggesting potential colon-targeted drug delivery applications. *Ex vivo* tests demonstrated that the medicated fiber mats could enhance the transmembrane of DS. Based on coaxial electrospinning, a new strategy is successfully developed for creating medicated nanomaterials.

1. Introduction

During the past several decades, more and more nano-drug delivery systems (DDS) have become commercial products. These products include polymeric nanoparticles, nanoliposomes, solid lipid nanoparticles, and microemulsions, which are partially fabricated using top-down methods based on the exploitation of mechanical forces, such as milling, high-pressure homogenization, and spray [1–3]. Most recently, the usage of electrostatic energy is drawing increasing attention for creating nanoproducts, such as electrospinning, electrospraying, and e-jet printing, which is termed electrohydrodynamic atomization (EHDA) in total. Because liquids can easily interact with electric fields, thus these methods are frequently exploited to remove solvents directly from the solutions to dry and solidify the micro-fluid jets, meanwhile generating micro/nanosize fibers or particles [4, 5].

Although EHDA methods are widely investigated for developing functional nanomaterials, their mechanisms are still unclear. Often a series of different factors would play their roles in influencing the process and in turn the created nanoproducts. These factors are clear to researchers and can be divided into three categories: (i) operative parameters such as applied voltages, tip-to-collector distance, and fluid flow rate; (ii) environmental conditions such as temperature, humidity, and vacuum; and (iii) the physicochemical properties of working fluids such as surface tension, conductivity, and viscosity. In the traditional single-fluid electrospinning, nanofiber fabrication and dimension control by these parameters have been well investigated for various polymers depending on their categories and the desired applications [6–9]. Although the reported methods are useful to a certain polymer, the size-reducing effect is limited and the implementation conditions are strict. For example, when a polymer concentration is utilized to decrease fiber's diameter, its narrow electrospinnable window would limit the effect; when an additive (such as a surfactant or a salt) is doped into

a polymer solution for downsizing, it may be infeasible due to lacking codissolving solvent or enough solubility.

During the past several years, double-fluid electrospinning (such as coaxial and side-by-side processes) and even multiple-fluid electrospinning (such as triaxial processes) have been reported in literature [10–13]. In these processes, an unspinnable fluid can be treated simultaneously with the electrospinnable polymeric fluids for carrying out double-fluid or multiple-fluid processes and creating nanostructures. Based on this new conception, Yu et al. developed the modified coaxial and triaxial electrospinning processes, which are characterized by the unspinnable outer fluids [9, 14, 15]. These modified processes have been utilized to coat nanofibers with Ag nanoparticles for antibacteria applications [14], to retard initial burst release of drug from medicated nanofibers [15]. With the usage of an unspinnable sheath liquid to conduct a coaxial process, the electrospun nanofibers' diameter can be manipulated in a controlled manner because the sheath fluid often has little influence on the properties of core spinnable polymeric solution. This simple relationship makes the diameter of nanofiber from core polymeric solution able to be adjusted by only one of the parameters of sheath fluid under a certain electrospinning condition. For example, it is reported that polyacrylonitrile nanofibers' diameters were able to be manipulated by the concentrations of LiCl in the sheath solution through a power equation [9]. However, frequent change of sheath fluids is not convenient but time-consuming. Provided the flow rate of sheath fluid can be taken as a key factor for manipulating nanofibers' size, it should be more facile because all need is to press the syringe pump for driving the sheath fluid.

The commencement of an electrospinning process is regarded as the balance of electrical forces and surface tensions. According to the following equation, the increase of conductivity and decrease of surface tension of working fluid should provide new protocols for carrying out an electrospinning process more stably and robustly [16]:

$$V_c \sim \sqrt{\frac{\gamma d^2}{\varepsilon R}}, \tag{1}$$

where V_c is the critical voltage for a jet emanating from the meniscus tip, d is the nozzle-to-collector distance, ε is the permittivity, γ is the surface tension, and R is the principal curvature of the liquid meniscus. Electrons are easy to aggregate on the surface of working fluid [17]. Thus in the coaxial electrospinning, it is often the physical and chemical properties of the shell fluid that determine an electrospinning process. According to the equation, an increase of conductivity (ε) and a decrease of surface tensions (γ) would mean that only a small applied voltage (V_c) was needed to initiate a coaxial electrospinning process.

Here, a salt solution is exploited as a shell working fluid, and the influence of its flow rate on both the electrospinning process and the quality of final nanofiber product is investigated in detail. Different from traditional coaxial electrospinning, in which the shell fluid must be electrospinnable, the modified coaxial processes can exploit a wide series of liquids as the shell working fluids regardless of their electrospinnability (solvent, solutions of little molecules, dilute polymer solutions, and even suspensions and emulsions) [14, 15]. Thus this new modified coaxial process can even expand the capability of electrospinning to create nanomaterials and nanostructures for realizing a series of new possibilities in the field of functional nanomaterials.

In the area of nanomedicine, the polymeric nano-DDS are mainly in the form of nanoparticles (NPs). However, for oral administration, the major and the most favorite way for the patients, electrospun nanofiber-mat-based DDS should have some special advantages over NPs besides the facile, simple, and straightforward fabrication processes using electrospinning [18, 19], such as easy aftertreatment and easy formation transitions from the randomly assembled or aligned fiber mats. Their unique characteristics (diameter in the nanoscale but length in the macroscopic scale) would endow them having the merits possessed by both the NPs DDS at nanoscale in altering the biopharmaceutical and pharmacokinetic properties of the drug molecule for favorable clinical outcomes and also those possessed by the conventional solid dosage forms such as easy processing, good drug stability, and ease of packaging and shipping [20–22].

Based on the above-mentioned knowledge, we developed modified coaxial electrospinning to produce drug-loaded Eudragit® L100 (EL100) nanofibers for potential colon-targeted delivery of diclofenac sodium (DS). A salt (NaCl) solution was exploited as the shell working liquid and its flow rate was exploited as a regulatory factor. EL100, a pH-sensitive methacrylate-based copolymer developed by Röhm Company in Germany, has been widely used for the colon-targeted formulation development in pharmaceutical industry and laboratory, such as tablet coating, tablet matrix, microspheres, and nanoparticles [23].

2. Materials and Methods

2.1. Materials. Eudragit L100 (EL100, average molecular weight approximately 135,000 Da) was purchased from Röhm GmbH & Co. KG (Darmstadt, Germany). Analytical grade N,N-dimethylacetamide (DMAc) and ethanol were provided by the Sinopharm Chemical Reagent Co., Ltd. (Shanghai, China). Sodium chloride was of analytical grade and obtained from Shanghai Shiyi Chemical Reagent Co., Ltd. (Shanghai, China). All other chemicals are of analytical grade and used as received. Water was double distilled just before use.

2.2. Coaxial Electrospinning. The spinning solutions of EL100 were prepared by dissolving 14.0 g EL100 and 2.0 g DS in 100 mL ethanol. The shell solution consisted of 0.1 g NaCl in a 100 mL mixture of DMAc and ethanol (20 : 80, v : v). Two syringe pumps (KDS200, KDS100, Cole-Parmer, USA) and a high-voltage power supply (ZGF 60 kV/2 mA, Shanghai Sute Corp., China) were used. The applied voltage was fixed at 14 kV. The fibers produced were collected on an aluminum foil at a distance of 20 cm. A homemade concentric spinneret was

exploited in both the single-fluid and the modified coaxial processes.

The flow rate of core EL100 fluid was kept at 1.0 mL/h. When the shell fluid was switched off, it was single-fluid electrospinning with the inner capillary as a spinneret. When the pump loaded with the syringe containing the salt solution was switched on to push the shell fluid, it was a modified coaxial electrospinning process. The flow rate of shell solution was exploited as a controlled factor. Experiments were recorded using a digital camera (PowerShot A640, Canon, Japan) under 11x magnifications.

2.3. Morphology. The surface morphology of electrospun fibers and raw DS powders were assessed using a JSM-5600LV scanning electron microscope (SEM, Japan Electron Optics Laboratory Co. Ltd.). Prior to the examination, the samples were gold sputter-coated under nitrogen atmosphere to render them electrically conductive. The average fiber diameter was determined by measuring diameters of fibers at over 100 times over some different fibers in the FESEM images using ImageJ software (National Institute of Heath, Bethesda, MD, USA).

2.4. Physical Forms of the Components and Their Compatibility. X-ray diffraction (XRD) analyses were performed using a D/Max-BR instrument with a diffractometer (RigaKu, Tokyo, Japan). The measurements were conducted under CuKα (λ = 1.541 Å), 40 kV, and 30 mA as X-ray source with Kb 142 (Ni) filter. The raw materials (EL100 and DS), their physical mixture (consisting of EL100 and DS in a weight ratio of 7 : 1), and the electrospun nanofibers were measured for angles 2θ between 5° and 60°.

Attenuated reflectance Fourier transform infrared (ATR-FTIR) tests were carried out using a Perkin-Elmer Precisely Spectrum One FTIR Spectrometer with Universal ATR Sampling Accessory (Perkin 135 Elmer, USA). 10 mg of sample (raw DS and EL100 powders, their physical mixture, and the medicated nanofibers) was placed on the diamond surface plate to be scanned. The scanning range was 500–4000 cm^{-1} at an average of 8 scans and the resolution of 2 cm^{-1}.

2.5. Functional Performance. A standard equation was built for measuring the content of DS in the unknown samples with phosphate buffered saline (PBS, 0.1 N, pH = 7.0) as the solvent of pure drug using a UV spectrophotometer (UV-2102PC, Unico Instrument Co. Ltd., Shanghai, China). To determine drug loading efficiency (LE), 100 mg of electrospun nanofibers was added to 10 mL of 10% ethanol aqueous solution to extract all the loaded DS. Then the solutions were diluted using PBS to a suitable concentration for UV measurement. The LE was calculated using the following equation:

$$\text{LE}\,(\%) = \frac{(\text{DS weight measured})}{(\text{DS weight calculated from the preparation})} \times 100\%. \quad (2)$$

The *in vitro* dissolution experiments were performed according to the *Chinese Pharmacopoeia* (2015 Ed.) Method II. This paddle method was executed on a RCZ-8A dissolution apparatus (Tianjin University Radio Factory, Tianjin, China). Samples (0.2 g of electrospun nanofibers and the physical mixture) equivalent to 25 mg of DS were added directly in the dissolution vessel containing 900 mL dissolution liquid (in the first two hours, 0.01 N HCl was used; later, 0.36 g NaOH was added to the dissolution media to neutralize them). The temperature was maintained at 37 ± 1°C and it was stirred at 50 rpm. At predetermined time points, samples of 5.0 mL were withdrawn from the dissolution medium and replaced with 5.0 mL fresh PBS to maintain a constant volume. After filtration using a 0.22 μm membrane (Millipore, Billerica, MA, USA) and appropriate dilution with PBS, samples were analyzed by UV spectroscopy at λ_{max} = 276 nm. All measurements were repeated six times. Percentage of dissolution was readily calculated according to the calibration standard equation of DS.

The *ex vivo* permeation studies were performed using a RYJ-6A diffusion test apparatus (Shanghai Huanghai Drug Control Instrument Co., Ltd.), in which materials were mounted in six Keshary-Chien glass diffusion cells and a water bath system maintained a constant temperature of 37 ± 0.2°C. Each cell had a diffusion area of 2.60 cm^2, and the receptor compartment had a capacity of 7.2 mL PBS. Each donor compartment was filled with 1 mL PBS and the hydrodynamics in the receptor compartment were maintained by stirring with a Teflon coated magnetic bead at 50 rpm. Large intestines were obtained from pigs after slaughtering (Baoshan Jiangwan slaughterhouse, Shanghai, China). The intestine was washed carefully with physiological saline solution (NaCl 0.9% w/v) to remove nondigested food. The biomembranes peeled off from the intestines were fixed on the diffusion cells with the mucosal walls upward. They were equilibrated for 30 min before permeation tests.

Physical mixture of EL100 and DS and nanofibers F2 and F4 (100 mg) were placed on the biomembrane surface. Samples (1 mL) were withdrawn from the receptor compartment at timed intervals and 1 mL fresh PBS was compensated. The samples were filtered through a 0.22 μm membrane (Millipore, USA). The absorption of filtrate was measured at 276 nm to determine DS presented in the water phase. All the measurements were carried out in triplicate.

3. Results and Discussion

3.1. Modified Coaxial Electrospinning. A schematic diagram of the modified coaxial electrospinning is shown in Figure 1(a). Just as a traditional coaxial electrospinning system and also a single-fluid electrospinning system, the modified coaxial electrospinning system consists of four components to exploit the electrostatic force: a power supply, one or two syringe pumps, a fiber collector, and a spinneret. The spinneret is the most important part in a system. It not only provides a template for creating structural nanofibers (such as core-shell and side-by-side), but also determines how many working fluids are needed during the process and correspondingly the needed syringe pumps.

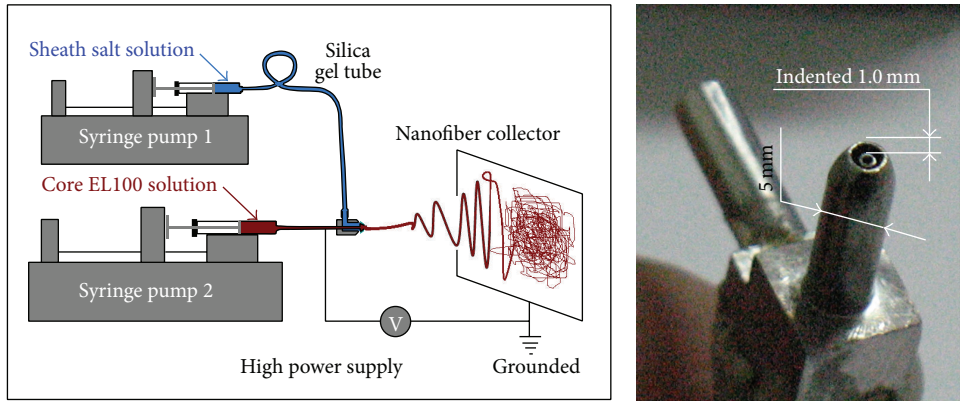

Figure 1: Modified coaxial electrospinning with a salt solution as shell fluid: (a) a schematic diagram shows the components of a modified coaxial electrospinning system; (b) a digital picture of the homemade concentric spinneret.

Table 1: Parameters of the electrospinning processes and their products.

Number	Process[a]	Shell-to-core fluid flow rate ratio	Morphology[b]	Diameter[c] (μm)
F1	Single	0	Linear	1.43 ± 0.56
F2	Coaxial	0.05	Linear	0.91 ± 0.23
F3		0.1	Linear	0.75 ± 0.10
F4		0.2	Linear	0.46 ± 0.12
F5		0.3	Linear with a few spindles	0.28 ± 0.14
F6		0.5	Mixed	—

[a]A fixed core fluid flow rate of 1.0 mL/h was exploited.
[b]"Linear" morphology refers to fibers with few beads or spindles and "mixed" morphology refers to nanofibers with beads, spindles, and clumps.
[c]Expressed as the mean ± SD of over 100 fiber diameter measurements.

A digital picture of the homemade concentric spinneret exploited in the present study is shown in Figure 1(b). According to reports in literature, in a concentric spinneret, the reasonable design should be a one in which the inner capillary often projected slightly out the outer capillary. These characteristics help to prevent diffusion and mixture of the core and shell liquids during the electrospinning process. However, here the upper surface of the nozzle of inner capillary was designed to be indented 1.0 mm from the tip of the outer capillary. This should facilitate easier envelopment of the core working fluid by the shell salt solution.

At all the experiments, the core fluid flow rate was fixed at 1.0 mL/h. The shell-to-core fluid flow rate ratio was exploited as a controlled factor to manipulate the electrospinning processes. Six types of fibers were fabricated with the flow rate of shell NaCl solutions increased from 0 to 0.05, 0.1, 0.2, 0.3, and 0.5 mL/h, and they were denoted as F1, F2, F3, F4, F5, and F6, respectively (Table 1).

3.2. The Influence of the Shell Salt Solutions on the Modified Coaxial Processes. Observations of the electrospinning processes for preparing F1 and F3 to F6 and the arrangement of the apparatuses are shown in Figure 2. The spinneret was horizontally placed and connected with the syringe pump driving the core EL100 solution. The shell salt solution driven by another pump was connected with the spinneret through high elastic silica tubing. The collector, a cardboard wrapped with an aluminum foil, was vertical and kept a 20 cm distance from the nozzle of the spinneret. Both the connections between the high power supply and the spinneret and the grounded line and fiber collector were alligator clips (Figure 2(a) and its inset).

Regardless of one fluid or double fluids, the single-fluid and coaxial electrospinning would experience the three steps similarly, that is, the formation of Taylor cone, the emission of a straight fluid jet from the Taylor cone, and the bending and whipping instable region. However, the single-fluid electrospinning of core EL100 solution was very easy to be clogged due to the formation of semisolid substance around the spinneret (Figure 2(b)). Thus manual removal of the substance was needed now and then to ensure a continuous preparation of fibers F1. This phenomenon should have a close relationship with the easy evaporation of ethanol and the strong interactions between EL100 molecules and the metal spinneret. When there was shell fluid, despite only a small shell-to-core fluid flow rate ration of 0.05 for the preparation of fiber F2, the clogging phenomena were greatly decreased and the straight fluid jets had a variable length. When the flow rate of shell fluid was increased to 0.1 mL/h for producing fibers F3, the modified coaxial electrospinning could run continuously and stably with an embedded Taylor cone and a long straight fluid jet of 35 mm (Figure 2(c) and its

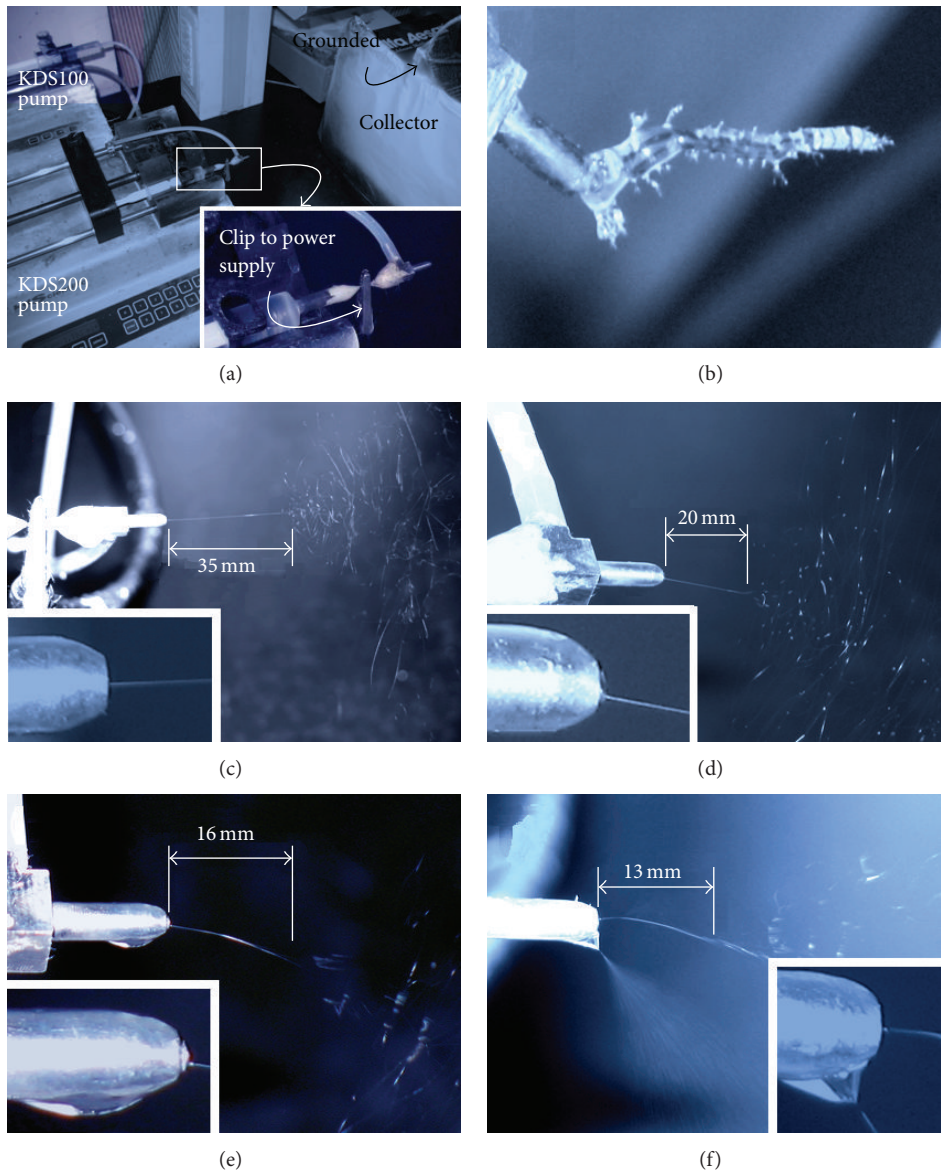

FIGURE 2: Observations of the electrospinning processes: (a) a digital picture showing the arrangement of apparatuses of the modified coaxial electrospinning system, the bottom-right inset showing the connection of the spinneret with power supply using an alligator clip; (b) a digital picture showing the clogging phenomenon during the single-fluid electrospinning of core EL100 solution; ((c)–(f)) digital pictures showing the production of F3 to F6 using the modified coaxial electrospinning under a shell-to-core fluid flow rate ratio of 0.1 to 0.2, to 0.3, and to 0.5, respectively. The applied voltage was fixed at 14 kV. The left-bottom insets show an enlarged view of the Taylor cone corresponding to the modified coaxial processes.

inset, Table 2). The increase of shell fluid flow rate to 0.2 mL/h and 0.3 mL/h resulted in a similar process, but with a shorter straight fluid jet of 20 mm and 16 mm (Figures 2(d) and 2(e), Table 2) and a discerned Taylor cone (the inset of Figures 2(d) and 2(e)).

With further increase of the shell fluid flow rate to 0.5 mL/h, there were often two separate EHDA processes that happened at the nozzle spinneret (Figure 2(f) and its inset, Table 2). One was still an electrospinning process with a straight fluid of 13 mm, and the other was a typical electrospraying process. The shell solution had a better conductivity but a smaller viscosity than the core fluid and maybe also some action of the gravity of the shell fluid; the division of the core EL solution and shell NaCl solution was inevitable when an excessive shell fluid was driven out. Thus for a stable and robust modified coaxial electrospinning process, a reasonable selection of shell fluid flow rate is very important.

3.3. Morphology of Fibers and Their Size Distribution. Just as anticipated, fibers F1 fabricated using single-fluid electrospinning of the core EL100 solution show a complicated

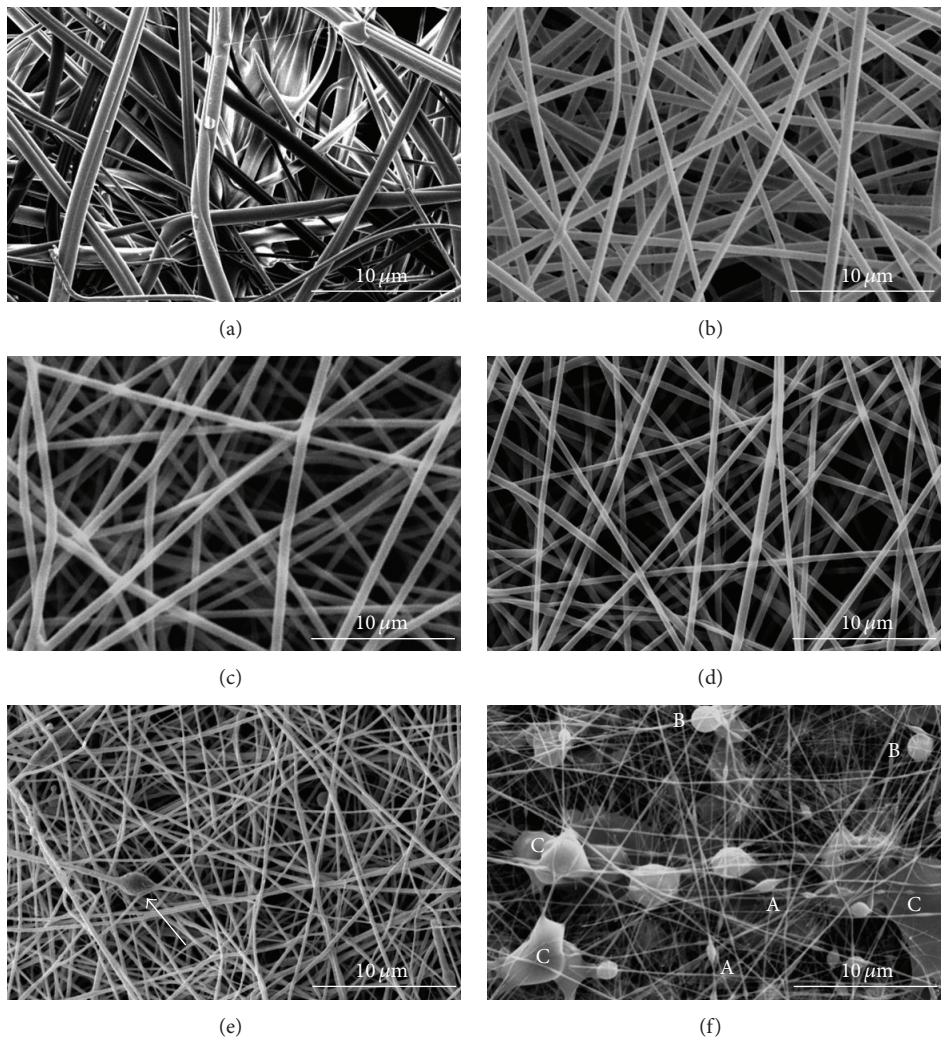

Figure 3: FESEM images of the medicated nanofibers: (a) F1, (b) F2, (c) F3, (d) F4, (e) F5, and (f) F6.

Table 2: The different behaviors of working fluids under different shell fluid flow rate.

Number	Process	F^a	Taylor cone	Straight fluid jet[b]	Instable region
F1	Single	0	Clogging	Varied	Discontinuous bending and whipping
F2	Coaxial	0.1	Indented	35 mm	Continuous and stable bending and whipping
F3		0.2	Smaller	20 mm	Continuous and stable bending and whipping
F4		0.5	Double	13 mm	A combination of spraying and spinning

[a] F refers to sheath-to-core fluid flow rate ratio.
[b] The values are estimated according to the size of spinneret shown in Figure 1(b).

morphology (Figure 3(a)). Some large fibers showed a "side-by-side" topography. The quick evaporation of solvent from the surface of fluid jets generated solid skin on the fibers firstly; later the escape of trapped solvent in the inner part of fibers and the barometric pressure deformed the fibers to form a concave on their surface. The randomly collected fibers distributed ununiformly and some fibers are several times larger than others, reflecting a poor size distribution. In sharp contrast, fibers F2, F3, and F4 show a uniform distribution with all of them exhibiting a linear morphology. No beads-on-a-string or spindles-on-a-line morphology occurs. Also no particles can be discerned on the surface of fibers, suggesting no solid phase separation during the electrospinning processes (Figures 3(b), 3(c), and 3(d)). However, when an abundant shell fluid was pumped during the coaxial processes, nanofibers F5 have some spindles on them (as indicated by the arrow in Figure 3(e)). When excessive shell fluid was provided, nanofibers F6 exhibited a mixed

morphology (Figure 3(f)). Not only do many beads-on-a-string/spindles-on-a-line morphologies occur (as indicated by "A" in Figure 3(f)), but also round particles (as indicated by "B" in Figure 3(f)) and even large clumps (as indicated by "C" in Figure 3(f)) can be found in the fiber mat. During the division of shell and core fluids (Figure 2(f)), the shell solutions should "rob" some EL100 and DS from the core liquid. Thus the core solution with a lower concentration than the original value experienced an electrospinning process to form the spindles-on-a-line morphology, whereas the shell fluids were subjected to an electrospraying process with varied concentrations of the solutes, which in turn resulted in the particles and clumps on the fiber mats.

The diameters' distributions of fibers F1 to F5 are shown in Figures 4(a) to 4(e). Obviously, fibers from the coaxial processes have a finer diameter value and a more homogeneous size distribution ($0.91 \pm 0.23\,\mu$m in Figure 4(b) for fibers F2, $0.75 \pm 0.10\,\mu$m in Figure 4(c) for fibers F3, $0.46 \pm 0.12\,\mu$m in Figure 4(d) for fibers F4, and $0.28 \pm 0.14\,\mu$m in Figure 4(e) for fibers F5) than fibers F1 from the single-fluid electrospinning ($1.43 \pm 0.56\,\mu$m in Figure 4(a)). The single-fluid electrospinning can be regarded also as a modified coaxial process, in which the shell fluid flow rate was 0 mL/h. The relationships between the fibers' diameter and the shell-to-core fluid flow rate ratio are exhibited in Figure 4(f). Regressed using power function, a scaling law of $D = 0.174F^{-0.579}$ ($R^2 = 0.9877$) can be built, which shows better relativity than a regressed linear equation $D = 1.017 - 2.571F$ ($R^2 = 0.9241$) within an F range of 0 to 0.3. Thus the power function equation can be used to predict the diameters of nanofibers fabricated using the coaxial processes within a suitable range of shell solutions' flow rates.

Right after the reviving of electrospinning around 1995, researchers are always looking for new ways for generating nanofibers with tunable diameters. Based on the single-fluid electrospinning, operative parameters, environmental conditions, additives, and also the physical and chemical properties of working fluids have been exploited to exert active influence on the reduction of the nanofibers [24–26]. However, the results were far from satisfactory. The aim of obtaining ultra-thin nanofibers is often compromised by the detriment of nanofiber quality when a single-fluid process is exploited. This is due to the complicated electro-fluid-mechanical property of the electrospinning process and often the filament-forming polymer only having a narrow electrospinnable window. Here, with salt solutions as shell fluids, the coaxial process can be used to fabricate nanofibers in a controllable approach.

A diagram of the mechanism about the sheath fluid flow rate on the formation of polymeric nanofibers is shown in Figure 5. Compared with the electrical force (E) applied on the working fluids, the gravity (G) is often very small and can be neglected [9]. The sheath fluid exerts its influence mainly in the regions of "A" Taylor cone and "B" bending and whipping and in turn the final products in region "C." When there is no sheath fluid, a standard single-fluid electrospinning process can create fibers from the electrospinnable polymeric solutions. When evaporative solvent is utilized to prepare the solution, clogging easily occurs. When a sheath fluid is exploited, it can lubricate the spinneret and provide a liquid protection to prevent the formation of semisolid substance on the surface of fluid jets. Within a suitable range of sheath-to-core fluid flow rate ratio, the increase of sheath fluid flow rate would keep the bending and whipping jets in a fluid state for a longer time to be subjected to the drawing from the electrical forces. Thus fibers with smaller diameter can be achieved. This mechanism is obviously different from a previous publication in which LiCl solution was used as sheath fluid to fabricate polyacrylonitrile nanofibers, where the strategy is to increase LiCl concentrations and thus elevate the electrical drawing forces [9]. Certainly, excessive sheath fluid flow rate would result in the division of Taylor cone and the formation of products with mixed morphology.

3.4. Physical Form and the Compatibility between Components. As shown in Figure 6(a), the XRD patterns of DS have many sharp peaks, reflecting that the drug is essentially a crystalline material. The XRD pattern of EL100 shows a hump, indicating that it is an amorphous polymeric matrix. Just as anticipated, the physical mixture of drug and polymer has sharp peaks in its XRD patterns. In contrast, there are not any drug peaks occurring in the patterns of fibers F2 and F4. Thus it can be concluded that the coaxial process had altered the drug physical status from crystalline form to an amorphous form with the polymeric matrix.

The ATR-FTIR spectra of raw materials, their physical mixture, and nanofibers F2 and F4 are shown in Figure 6(b). DS has a characteristic peak at 1577 cm^{-1}, which should be attributed to the C=C stretch vibration of phenyl groups. EL100 has a characteristic band at 1734 cm^{-1} due to C=O stretch vibration of carbonyl groups. Both of these two above-mentioned characteristic peaks occur in the spectra of physical mixture, reflecting that few interactions happen between the double components in the mixture. However, the characteristic bands of both DS and EL100 disappear in the spectra of nanofibers F3, but a new band of 1691 cm^{-1} occurs. According to the molecular structure of DS and EL100, this change should be attributed to the formation of hydrogen bonds between them.

The solidification from fluid jets to solid nanofibers during the electrospinning process is very quick, often on a time scale of 10^{-2} s. Thus it is thought that the physical forms of the components in the solutions are able to be propagated into the medicated nanofibers after electrospinning [27]. Provided favorable secondary interactions exist between them, the drug and carrier can coexist or mix in a molecular way, which can effectively retard the recrystallization of DS. Thus the medicated nanofibers from the coaxial process are essentially solid dispersions or nanocomposites.

3.5. Functional Performance. A UV scan of the DS solution containing 20 μg/mL is shown in the inset of Figure 7(a). DS has a maximum absorbance at 276 nm. Thus this wavelength was exploited to build the standard equation, which is expressed as $A = 0.0082 + 0.0323C$ ($R = 0.9991$) within

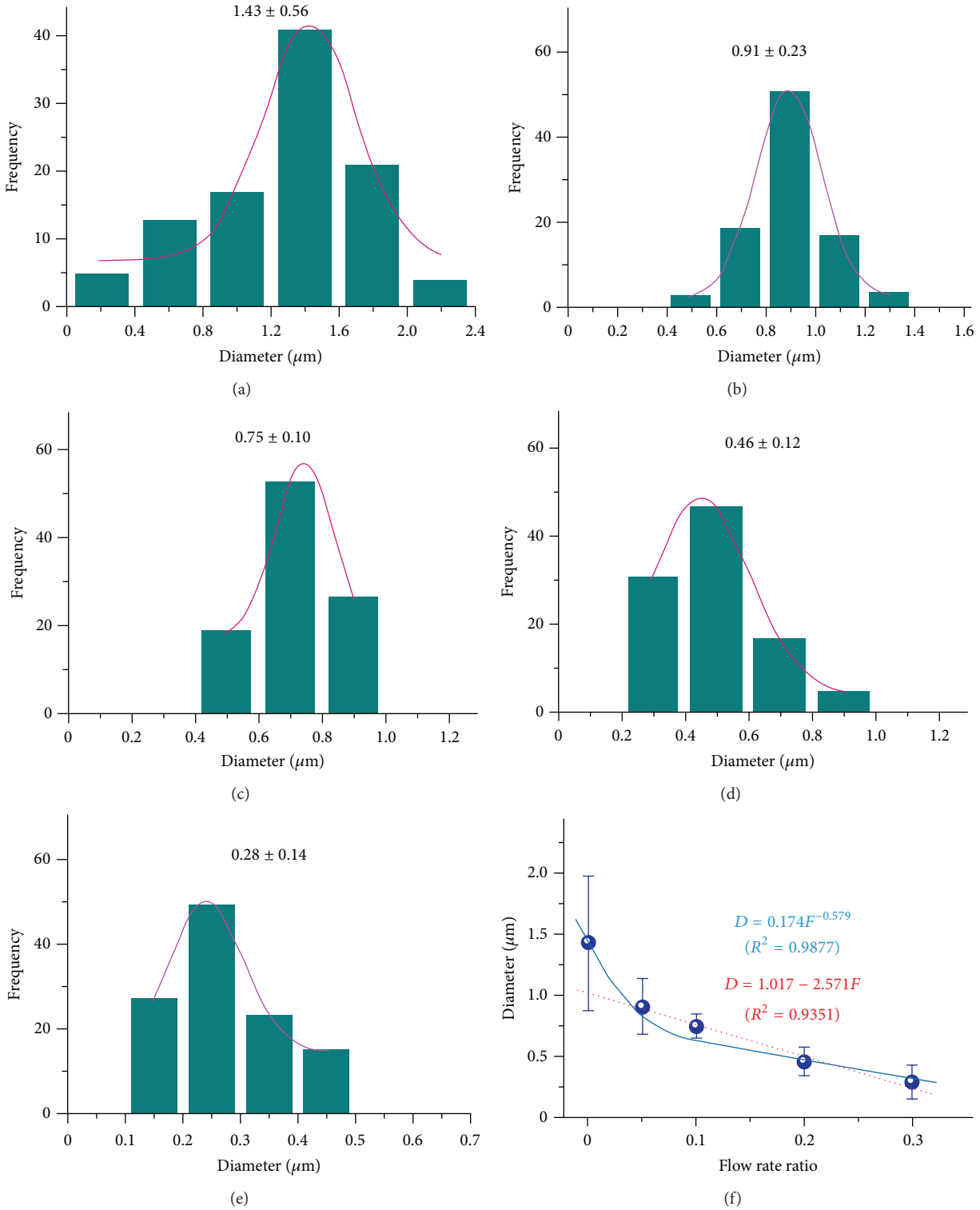

Figure 4: The influence of shell salt solutions' flow rate on the size of medicated fibers: ((a)–(e)) diameter distribution of fibers F1 to F5; (f) the relationships between the fibers' diameter and the shell-to-core fluid flow rate ratio.

a linear range from 2 to 50 μg/mL in Figure 7(a). Six times of the detection of the drug content in the nanofibers is 12.2 ± 0.4%, almost the same with the calculated value according to the feed in preparation.

The drug *in vitro* release profiles of the electrospun medicated nanofibers F2 and F4 and the physical mixture are shown in Figure 7(b). Apparently, the medicated nanofibers have altered the drug release behaviors in two aspects. First,

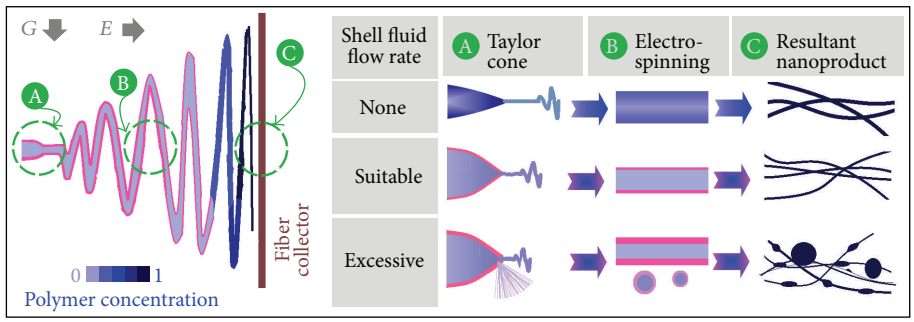

Figure 5: A diagram of the mechanism about the sheath fluid flow rate on the formation of polymeric nanofibers. G and E represent gravity and electrical force, respectively.

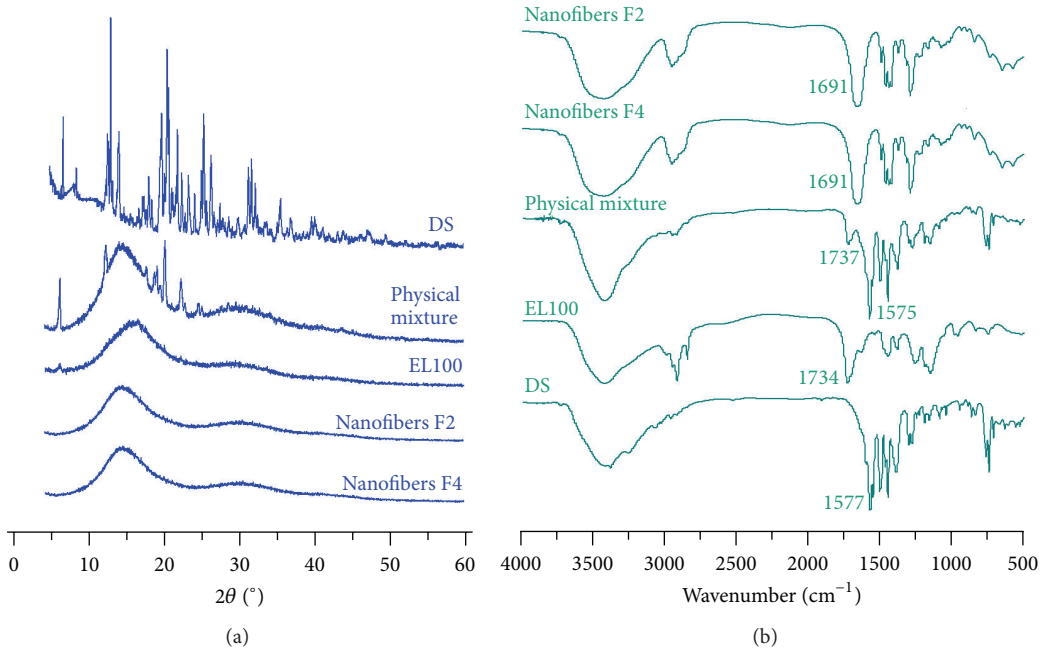

Figure 6: Physical forms of components and their compatibility in composite nanofibers: (a) XRD patterns; (b) ATR-FTIR spectra.

as a pH-sensitive polymeric matrix, EL100 has successfully retarded the drug release in an acid environment of pH = 2 at the first two hours. Second, the nanofibers prolonged the drug release time period in the neutral condition. Thus, these medicated nanofibers have the potential applications as oral drug delivery systems that provide a colon-targeted sustained release profile. Nanofibers F4 provided a better drug release profile than nanofibers F2 in that the former has a shorter time period of "tailing-off" release. Many commercial tablets are essentially a physical mixture of drug and polymeric carrier, which is expected to change the drug release behaviors through the polymers' physicochemical properties. However, the effect is often very limited because the physical state of drug is almost the same with the raw drug powders. Shown in Figure 7(c) are the FESEM images of raw DS particles. In the commercial tablets, DS still presents in a cubic crystal format. However, when DS was encapsulated into EL nanofibers, the DS molecules would disperse in the polymeric matrix in an amorphous state (Figure 7(d)). Accompanied with the polymer physical entanglements, the favorable drug-polymer interactions would play their roles in keeping the stability of the drug-polymer nanocomposites. Thus in the acid condition, the insoluble property of EL100 would protect the loaded DS molecules to retard its release. And in the neutral condition, the slow dissolution of EL100 would gradually release the contained DS in a sustained manner. With the same raw materials, electrospun medicated nanofibers were able to provide a better drug controlled release profile. Thus a more effective drug absorbance and a longer therapeutic blood concentration can be expected after oral administration.

The results of permeation tests on colon membrane are shown in Figure 8. After 12 h, 3.92 ± 0.59, 7.85 ± 0.81, and 8.24 ± 0.73 mg of DS were transmitted into the receptor cells. Although, in the *in vitro* tests, the physical mixture released DS faster than nanofibers F2 and F4, the nanofibers could promote double permeated DS molecules through the colon membrane. This contradictory experimental result

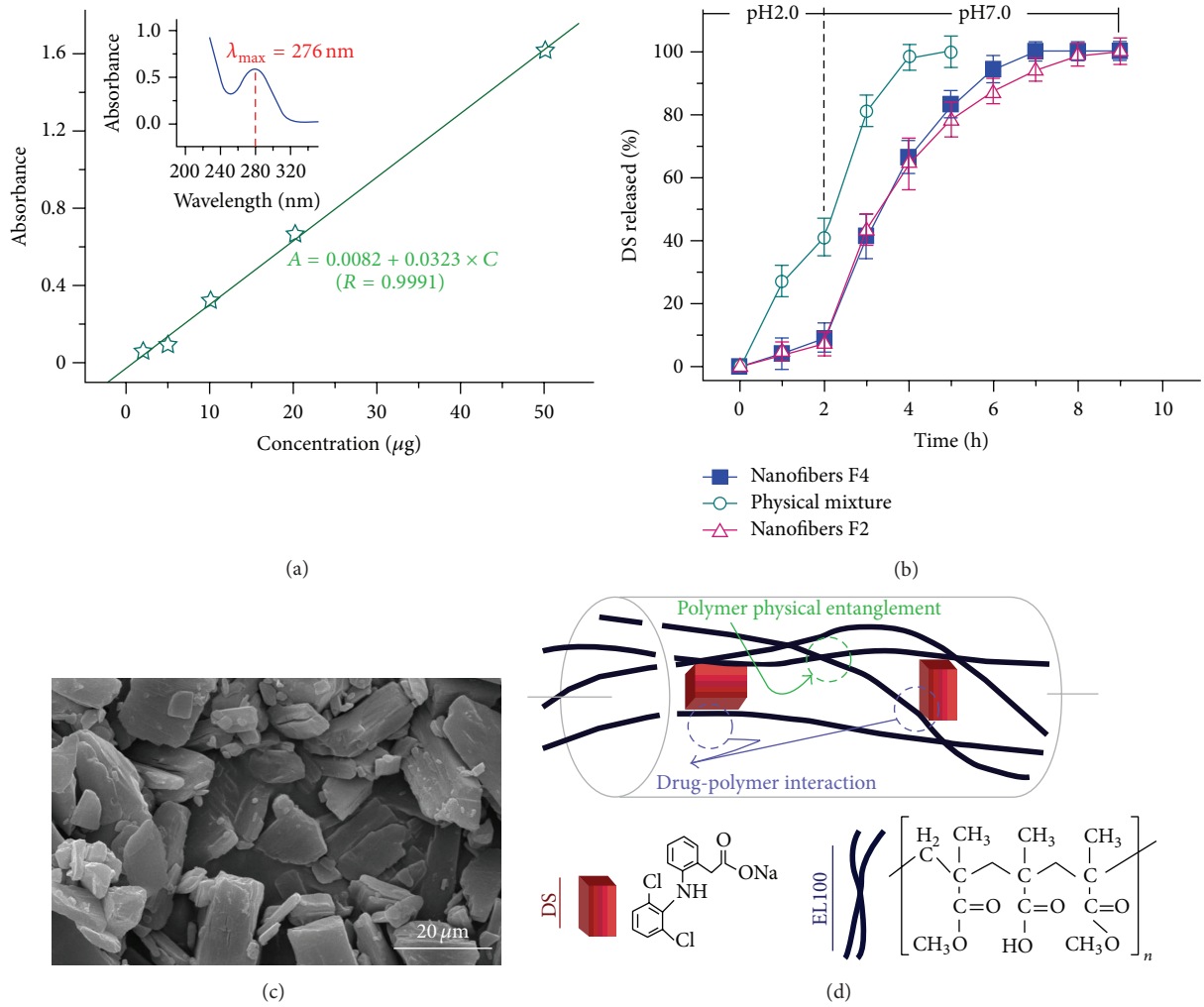

Figure 7: Functional performance of the composite medicated nanofibers: (a) the standard equation for the detection of DS using UV spectrophotometer; (b) the *in vitro* DS release profiles of nanofibers F2 and F4 and the control samples of physical mixture ($n = 6$); (c) FESEM images of the raw DS particles; (d) a diagram of the distribution of DS molecules in their polymeric matrix.

should be attributed to the different physical state of DS; its amorphous state in the nanofibers made DS molecules easy to be dissolved and permeate through the membrane in the donor cell with very limited dissolution media. In sharp contrast, the crystalline DS powders were difficult in dissolution and permeation when they were put on the colon membrane in the donor cells. Nanofibers F4 showed slightly better permeation results than nanofibers F4, which have a larger diameter. By the way, for potential oral administration, the encapsulation of DS in polymeric carrier should alleviate the potential anaphylactic reaction of drug particles with the digestive tracts.

4. Conclusions

Modified coaxial electrospinning was successfully developed to promote the nanofabrication of medicated fibers, in which salt solutions were employed as sheath fluids. Based on the usage of a homemade concentric spinneret, coaxial electrospinning was implemented under different flow rates of shell solutions. A scaling law between the fibers' diameter (D, μm) and the shell-to-core fluid flow rate ratios (F) was built as $D = 0.174F^{-0.579}$ ($R^2 = 0.9877$). XRD and ATR-FTIR results demonstrated that the electrospun nanofibers were essentially nanocomposites, where the drug had fine compatibility with its polymeric carrier. The coaxial process would not result in drug loss during the preparation. *In vitro* tests verified that the medicated nanofibers were able to release the contained drug in a sustained manner in the neutral condition, appearing better functional performance than their physical mixture. *Ex vivo* permeation studies demonstrated that the nanofibers were able to provide a double permeated amount of drug through the colon membrane compared to the corresponding physical mixture. It is concluded that coaxial electrospinning with a salt solution as a sheath fluid comprises a facile process for producing medicated nanomaterials with tunable diameters and improved functional performance.

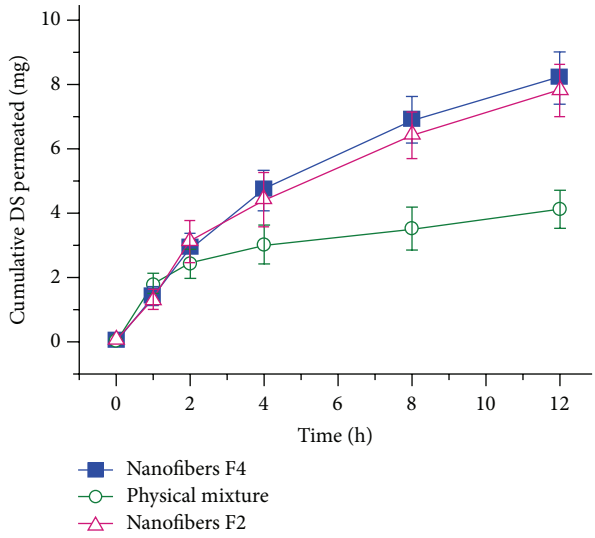

FIGURE 8: *Ex vivo* permeation tests of nanofibers F2 and F4 and the control samples of physical mixture on biomembrane ($n = 3$).

Competing Interests

The authors declare that they have no competing interests.

Acknowledgments

This work was supported by the Training Project for Excellent Young and Middle-Aged Backbone Teachers of Higher Schools in Guangxi province, the National Science Foundation of China (nos. 51373101 and 5140030478), and the College Student Innovation Project (Grants SH201510252167 and 20151025253).

References

[1] M. A. Alam, F. I. Al-Jenoobi, and A. M. Al-Mohizea, "Commercially bioavailable proprietary technologies and their marketed products," *Drug Discovery Today*, vol. 18, no. 19-20, pp. 936–949, 2013.

[2] S. Mitragotri, P. A. Burke, and R. Langer, "Overcoming the challenges in administering biopharmaceuticals: formulation and delivery strategies," *Nature Reviews Drug Discovery*, vol. 13, no. 9, pp. 655–672, 2014.

[3] E. Merisko-Liversidge and G. G. Liversidge, "Nanosizing for oral and parenteral drug delivery: a perspective on formulating poorly-water soluble compounds using wet media milling technology," *Advanced Drug Delivery Reviews*, vol. 63, no. 6, pp. 427–440, 2011.

[4] S. Chakraborty, I.-C. Liao, A. Adler, and K. W. Leong, "Electrohydrodynamics: a facile technique to fabricate drug delivery systems," *Advanced Drug Delivery Reviews*, vol. 61, no. 12, pp. 1043–1054, 2009.

[5] D. I. Braghirolli, F. Zamboni, G. A. X. Acasigua, and P. Pranke, "Association of electrospinning with electrospraying: a strategy to produce 3D scaffolds with incorporated stem cells for use in tissue engineering," *International Journal of Nanomedicine*, vol. 10, pp. 5159–5170, 2015.

[6] K. Siimon, K. Mõisavald, H. Siimon, and M. Järvekülg, "Increasing mechanical strength of electrospun gelatin nanofibers by the addition of aluminum potassium sulfate," *Journal of Applied Polymer Science*, vol. 132, no. 35, pp. 42431–42435, 2015.

[7] K. S. Liu, C. H. Lee, Y. C. Wang, and S. J. Liu, "Sustained release of vancomycin from novel biodegradable nanofiber-loaded vascular prosthetic grafts: in vitro and in vivo study," *International Journal of Nanomedicine*, vol. 10, pp. 885–891, 2015.

[8] T. J. Sill and H. A. von Recum, "Electrospinning: applications in drug delivery and tissue engineering," *Biomaterials*, vol. 29, no. 13, pp. 1989–2006, 2008.

[9] D.-G. Yu, P. Lu, C. Branford-White, J.-H. Yang, and X. Wang, "Polyacrylonitrile nanofibers prepared using coaxial electrospinning with LiCl solution as sheath fluid," *Nanotechnology*, vol. 22, no. 43, Article ID 435301, 2011.

[10] G. Chen, Y. Xu, D.-G. Yu, D.-F. Zhang, N. P. Chatterton, and K. N. White, "Structure-tunable Janus fibers fabricated using spinnerets with varying port angles," *Chemical Communications*, vol. 51, no. 22, pp. 4623–4626, 2015.

[11] S. Agarwal, A. Greiner, and J. H. Wendorff, "Functional materials by electrospinning of polymers," *Progress in Polymer Science*, vol. 38, no. 6, pp. 963–991, 2013.

[12] D. G. Yu, C. Yang, M. Jin et al., "Medicated Janus fibers fabricated using a Teflon-coated side-by-side spinneret," *Colloids and Surfaces B: Biointerfaces*, vol. 138, no. 2, pp. 110–116, 2016.

[13] D.-G. Yu, X.-Y. Li, X. Wang, J.-H. Yang, S. W. A. Bligh, and G. R. Williams, "Nanofibers fabricated using triaxial electrospinning as zero order drug delivery systems," *ACS Applied Materials and Interfaces*, vol. 7, no. 33, pp. 18891–18897, 2015.

[14] C. Yang, D. G. Yu, D. Pan et al., "Electrospun pH-sensitive core-shell polymer nanocomposites fabricated using a tri-axial process," *Acta Biomaterialia*, vol. 35, no. 15, pp. 77–86, 2016.

[15] D.-G. Yu, W. Chian, X. Wang, X.-Y. Li, Y. Li, and Y.-Z. Liao, "Linear drug release membrane prepared by a modified coaxial electrospinning process," *Journal of Membrane Science*, vol. 428, pp. 150–156, 2013.

[16] L. Y. Yeo and J. R. Friend, "Electrospinning carbon nanotube polymer composite nanofibers," *Journal of Experimental Nanoscience*, vol. 1, no. 2, pp. 177–209, 2006.

[17] O. Salata, "Tools of nanotechnology: electrospray," *Current Nanoscience*, vol. 1, no. 1, pp. 25–33, 2005.

[18] A. Balogh, T. Horváthová, Z. Fülöp et al., "Electroblowing and electrospinning of fibrous diclofenac sodium-cyclodextrin complex-based reconstitution injection," *Journal of Drug Delivery Science and Technology*, vol. 26, pp. 28–34, 2015.

[19] X. Li, M. A. Kanjwal, L. Lin, and I. S. Chronakis, "Electrospun polyvinyl-alcohol nanofibers as oral fast-dissolving delivery system of caffeine and riboflavin," *Colloids and Surfaces B: Biointerfaces*, vol. 103, no. 3, pp. 182–188, 2013.

[20] X. Li, L. Lin, Y. Zhu, W. Liu, T. Yu, and M. Ge, "Preparation of ultrafine fast-dissolving cholecalciferol-loaded poly(vinyl pyrrolidone) fiber mats via electrospinning," *Polymer Composites*, vol. 34, no. 2, pp. 282–287, 2013.

[21] Z. K. Nagy, A. Balogh, B. Démuth et al., "High speed electrospinning for scaled-up production of amorphous solid dispersion of itraconazole," *International Journal of Pharmaceutics*, vol. 480, no. 1-2, pp. 137–142, 2015.

[22] D.-G. Yu, Y. Xu, Z. Li, L.-P. Du, B.-G. Zhao, and X. Wang, "Coaxial electrospinning with mixed solvents: from flat to round Eudragit L100 nanofibers for better colon-targeted sustained drug release profiles," *Journal of Nanomaterials*, vol. 2014, Article ID 967295, 8 pages, 2014.

[23] V. Pornsopone, P. Supaphol, R. Rangkupan, and S. Tantayanon, "Electrospun methacrylate-based copolymer/indomethacin fibers and their release characteristics of indomethacin," *Journal of Polymer Research*, vol. 14, no. 1, pp. 53–59, 2007.

[24] H. Wen, C. Yang, D. Yu, X. Li, and D. Zhang, "Electrospun zein nanoribbons for treatment of lead-contained wastewater," *Chemical Engineering Journal*, vol. 290, no. 4, pp. 263–272, 2016.

[25] W. Klairutsamee, P. Supaphol, and I. Jangchud, "Electrospinnability of poly(butylene succinate): effects of solvents and organic salt on the fiber size and morphology," *Journal of Applied Polymer Science*, vol. 132, no. 43, pp. 42716–42726, 2015.

[26] T. Lin and X. Wang, *Encyclopedia of Nanoscience and Nanotechnology*, Edited by H. S. Nalwa, American Scientific, Los Angeles, Calif, USA, 2nd edition, 2011.

[27] W. Qian, D.-G. Yu, Y. Li, X.-Y. Li, Y.-Z. Liao, and X. Wang, "Triple-component drug-loaded nanocomposites prepared using a modified coaxial electrospinning," *Journal of Nanomaterials*, vol. 2013, Article ID 826471, 7 pages, 2013.